Submitted, 2015 Conference on Decision and Control (CDC)
http://www.cds.caltech.edu/~murray/papers/sm15-cdc.html

Quantitative Performance Bounds in Biomolecular Circuits due to Temperature Uncertainty

Shaunak Sen[1] and Richard M. Murray[2]

***Abstract*— Performance of biomolecular circuits is affected by changes in temperature, due to its influence on underlying reaction rate parameters. While these performance variations have been estimated using Monte Carlo simulations, how to analytically bound them is generally unclear. To address this, we apply control-theoretic representations of uncertainty to examples of different biomolecular circuits, developing a framework to represent uncertainty due to temperature. We estimate bounds on the steady-state performance of these circuits due to temperature uncertainty. Through an analysis of the linearised dynamics, we represent this uncertainty as a feedback uncertainty and bound the variation in the magnitude of the input-output transfer function, providing a estimate of the variation in frequency-domain properties. Finally, we bound the variation in the time trajectories, providing an estimate of variation in time-domain properties. These results should enable a framework for analytical characterisation of uncertainty in biomolecular circuit performance due to temperature variation and may help in estimating relative performance of different controllers.**

I. INTRODUCTION

Temperature is a global environmental variable that influences performance in a variety of engineering contexts. In electrical circuits, for example, transistor gains vary with temperature. Consequently, performance in larger circuits and devices, assembled from such components, also varies with temperature. Analogously, biomolecular circuit function can also be temperature-dependent, owing to the temperature-dependence of underlying reaction rate parameters. As robustness to temperature is often a performance objective for biomolecular circuits in both natural and design contexts, investigating the extent of variation in performance, due to a temperature uncertainty, is an important task.

For biomolecular circuits, such robustness analysis has been performed using tools from control theory [1]. These include the use of structured singular value analysis to characterize the robust stability of oscillations [2], [3], [4] as well as algorithms to generate robustness certificates for qualitative circuit behaviour to persist in presence of parametric uncertainty [5]. In addition to these, a robustness analysis approach commonly used has been Monte Carlo simulations — qualitative and quantitative characterisation of variation in circuit response through computer simulations, for a large set of randomly chosen points in the parameter space. Canonical examples of this approach are investigations in bacterial chemotaxis [6] and developmental pattern formation [7]. We have also previously used a similar approach to characterize uncertainty in performance of a variety of biomolecular circuits for a given temperature uncertainty [8], [9]. While conceptually easier, these simulations may be computationally expensive, unlike an analytic estimate.

There are three interesting aspects to consider about modelling uncertainty due to temperature in biomolecular circuits. One, due to the global nature of temperature variable, it should affect all reaction rate parameters. Typically, magnitudes of reaction rate parameters can increase by a factor of 2–3 for a $10^{\circ}C$ increase in temperature [10]. Two, in addition to the tracking and regulation problems, there can be a larger set of performance objectives in biomolecular circuits. Examples of quantitative objectives include, in addition to the steady-state and response-time robustness, the height and width of pulses, and, analogously, the amplitude and period of oscillations. Three, biomolecular circuits, being nonlinear systems in general, have an additional layer of complexity relative to the uncertainty modelling tools developed primarily in the context of linear systems. Indeed, even when the overall dynamical system model in biomolecular contexts is linear, various performance attributes such as steady-state value may be a nonlinear function of the parameters. Additionally, the components of the Jacobian matrix on linearisation around an operating point may themselves be a nonlinear function of reaction rate parameters. Given these, it is unclear how to obtain quantitative performance bounds in biomolecular circuits due to temperature uncertainty.

Here our objective is to analytically estimate performance bounds in biomolecular circuits due to temperature uncertainty. To address this, we use tools from control theory, apply them to biomolecular circuit outputs, developing a framework to represent uncertainty due to temperature. We investigate the variation in the steady-state value due to temperature uncertainty. Next, we linearise the system about the steady-state value, finding that temperature uncertainty can be represented as a feedback uncertainty and estimate bounds on the system transfer function magnitude. Finally, we bound the circuit trajectories, obtained either exactly or from the linearised dynamics, from which variation in time-domain properties such as pulse width and pulse height may be estimated. In all cases studied, we find that the analytical estimates performance bounds obtained, when assessed against Monte Carlo simulations, are reasonably good.

*Research supported in part by the Gordon and Betty Moore Foundation, the NSF Molecular Programming Project, and the Department of Science and Technology, Government of India.

[1]S. Sen is with the Department of Electrical Engineering, Indian Institute of Technology Delhi, New Delhi 110016, INDIA. shaunak.sen@ee.iitd.ac.in

[2]R. M. Murray is with the Divisions of Engineering and Applied Science, and Biology and Biological Engineering, California Institute of Technology, Pasadena, CA 91125, USA. murray@cds.caltech.edu

II. UNCERTAINTY IN STEADY-STATE VALUE

As primary determinants of cellular behaviour, biomolecular circuits participate in a range of dynamic functions, including signalling, differentiation, and oscillations. From a mathematical modelling point of view, one representation, in terms of ordinary differential equations, can be obtained based on mass action — the rate of reaction is proportional to the product of the concentration of the reactants, with the proportionality constant being the rate of the reaction,

$$\dot{x} = f(x, \mu), \tag{1}$$

where the variables (x) are concentrations of different biomolecules and the parameters (μ) are the reaction rate constants. In general, these parameters can depend on temperature T, $\mu = \mu(T)$. There are different performance features that might be of interest, both qualitative such as the stability of a steady-state, adaptation, and existence of limit cycles, as well as quantitative, such as the value of the steady-state, adaptation time, and the period of the limit cycle. Each of these is a function, possibly nonlinear, of the parameters, and consequently of temperature.

Consider the steady-state value x_0, which can be obtained as a solution to $\dot{x} = 0 \Rightarrow f(x_0, \mu) = 0$. This equation maps an uncertainty in the parameters, due to temperature uncertainty, into an uncertainty in the steady-state value. To obtain an analytical bound on the steady-state uncertainty, consider a linearisation around the steady-state value x_0 and a nominal parameter set μ_0,

$$\frac{\partial f}{\partial x}\Delta x + \frac{\partial f}{\partial \mu}\Delta\mu = 0 \Rightarrow \Delta x = A\Delta\mu, A = -\Big[\frac{\partial f}{\partial x}\Big]^{-1}\frac{\partial f}{\partial \mu},$$

if the inverse exists, with all partial derivatives evaluated at (x_0, μ_0). This equation may be used to estimate a performance bound for each of the components,

$$|\Delta x_{0i}| = |\sum_j a_{ij}\Delta\mu_i| \leq \sum_j a_{ij}|\Delta\mu_i|. \tag{2}$$

This upper bound on the absolute value of the uncertainty can be taken as an estimate of the variation in steady-state value.

To explore the utility of the performance bound obtained using the linearisation analysis, let us consider examples of biomolecular circuits. While these examples are simple, they recur in multiple contexts.

Example 1: Consider a simple mathematical model of gene expression, as a production-degradation process of a protein with concentration x,

$$\dot{x} = \alpha - \gamma x, \tag{3}$$

with a constant rate of production α and degradation, modelled as a first-order process, with rate constant γ. At steady-state, $x_0 = \alpha/\gamma$. Suppose $\alpha = \gamma = 1$, and when temperature increases by $10^\circ C$ each of the rates can change by a factor of 2–3. We choose nominal parameter values as $\alpha_0 = \gamma_0 = 2.5$ and their corresponding uncertainties as $\Delta\alpha/\alpha_0 = \Delta\gamma/\gamma_0 = \pm 1/5$. Nominal value of the steady-state value is $x_{00} = \alpha_0/\gamma_0 = 1$. Using the linearisation analysis above (Eqn. 2), we find that $|\Delta y| \leq |\Delta\alpha|/\gamma_0 + \alpha_0|\Delta\gamma|/\gamma_0 = 0.4$. We compared this analytical estimate with Monte Carlo simulations (Fig. 1a.) and find that the bounds are close to the actual variation. In particular, the upper bound underestimates the variation and the lower bound overestimates the variation. □

Example 2: Consider a simple mathematical model of a phosphorylable protein Z that can exist in two states, Z and Z^P. The phosphorylation and dephosphorylation reactions are first-order, and represented by rate constants k_+ and k_-, respectively. Using mass action, the rate of change of the fraction of phosphorylated protein, $x = Z^P/(Z + Z^P)$ can be obtained as,

$$\frac{dx}{dt} = k_+ - (k_+ + k_-)x. \tag{4}$$

At steady-state, $x_0 = k_+/(k_+ + k_-)$. Suppose that $k_+ = k_- = 10$ and there is a $10^\circ C$ increase in temperature. Because of this, the reaction rate parameters increase by a multiple of 2–3. To represent this parametric uncertainty, we may choose nominal parameter values as $k_{+0}/k_+ = k_{-0}/k_- = 2.5$ and uncertain parameter values as $\Delta k_+/k_{+0} = \Delta k_-/k_{-0} = \pm 1/5$. Due to this, the nominal steady-state $x_{00} = 1/2$ and, from above Eqn. (2),

$$\Delta x_0 \leq \frac{k_{+0}k_{-0}}{(k_{+0} + k_{-0})^2}\Big(\frac{|\Delta k_+|}{k_{+0}} + \frac{|\Delta k_-|}{k_{-0}}\Big) = \frac{1}{10}.$$

On comparing these with the Monte Carlo simulations, we find that the bounds cover the variation in steady-state value (Fig. 3b.). □

Example 3: Consider next a simple mathematical model of an Incoherent Feedforward Loop [11], a dynamic biomolecular circuit that is overrepresented in biomolecular circuit motifs [12], and capable of generating systems-level properties such as adaptation of the output y to step change in input u [13], fold-change detection to changes in u [14], [15], and pulsing output y [16],

$$\begin{aligned} \dot{x} &= \alpha_x u - \gamma x, \\ \dot{y} &= \alpha_y \frac{K_x}{x} u - \gamma y. \end{aligned} \tag{5}$$

The steady-state value of the output y is $y_0 = K_x\alpha_y/\alpha_x$. We had previously performed a robustness analysis of the steady-state around the parameters $\alpha_x = \alpha_y = K_x = \gamma = 1$ using Monte Carlo simulations [9], assuming that for a $10^\circ C$ increase of temperature the values of parameters α_x, α_y, and γ increase by a multiple of 2–3, while K_x, itself a ratio of two parameters, changes by a multiple 0.66–1.5. To represent this parametric uncertainty after the $10^\circ C$ increase in temperature, we can explicitly choose the nominal parameter values as $\alpha_{x0}/\alpha_x = \alpha_{y0}/\alpha_y = \gamma_0/\gamma = 2.5$, $K_{x0}/K_x = 1$ and the uncertainties as $\Delta\alpha_x/\alpha_{x0} = \Delta\alpha_y/\alpha_{y0}\Delta\gamma/\gamma_0 = \pm 1/5$, $\Delta K_x/K_{x0} = \pm 1/2$. For this, the nominal output $y_{00} = K_{x0}\alpha_{y0}/\alpha_{x0} = K_x\alpha_y/\alpha_x = y_0 = 1$. On performing

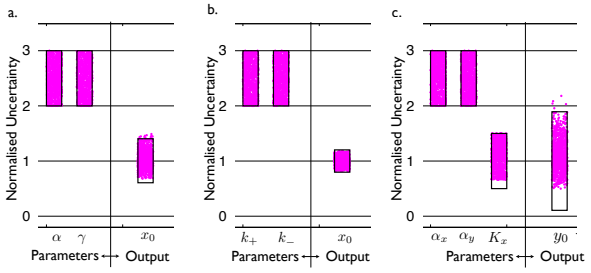

Fig. 1. Uncertainty bounds for steady-state for a. Production-degradation circuit model, b. Phosphorylation reaction, and c. Incoherent Feedforward Loop circuit model. Magenta dots represent the parameter choices and steady-state value calculations of a number of random simulations. Horizontal spread is for purposes of illustration. Black rectangular boxes represent the uncertainty bounds, assumed for the parameters or in the steady-state output obtained from the linearised analysis. The vertical axis is normalised uncertainty — variation in performance normalised to initial parameters specified.

the linearisation as in Eqn. (2), we get,

$$\begin{aligned}
\Delta y_0 &= \frac{K_{x0}}{\alpha_{x0}}\Delta\alpha_y + \frac{\alpha_{y0}}{\alpha_{x0}}\Delta K_x - \frac{K_0\alpha_{y0}}{\alpha_{x0}^2}\Delta\alpha_x, \\
\Rightarrow |\Delta y_0| &\leq \frac{K_{x0}}{\alpha_{x0}}|\Delta\alpha_y| + \frac{\alpha_{y0}}{\alpha_{x0}}|\Delta K_x| + \frac{K_0\alpha_{y0}}{\alpha_{x0}^2}|\Delta\alpha_x|, \\
\Rightarrow |\Delta y_0| &\leq \frac{9}{10}y_{00}.
\end{aligned}$$

We compared this bound with the variation in performance obtained from Monte Carlo simulations (Fig. 1c.). The upper bound underestimates the variation, although only slightly, for this set of parameters. In contrast, the lower bound overestimates the variation. □

Therefore, we find that this approach is helpful in analytically estimating of the performance uncertainty of the steady-state even though it is obtained from a standard linearisation-based analysis. Further, even though the presentation has been for a steady-state, variation in any function of the temperature-dependent parameters, such as a transient characteristic or an element of the Jacobian, can be usefully estimated in this fashion.

III. UNCERTAINTY IN LINEARISED DYNAMICS

As explicit solutions of nonlinear dynamical solutions are frequently unavailable, one way to analyse their dynamics is to first linearise the system equations around an operating point. In some cases, this approximation is the only practical means to study the dynamics. A reason for this may be the multiplicity of tools available to investigate the behaviour of linear systems, including for uncertainty representation. Typically, the basic idea for representing uncertainty is to split the components of the linearised system matrices into their nominal and uncertain components and to separate the uncertain components from the nominal system [1]. This provides an uncertainty representation of the linearised dynamics which is used to study robustness in stability and performance. In the present case, where temperature uncertainty affects all parameters, elements of the linearised system matrices can themselves be nonlinear combination of the operating point and the parameters, both of which can be temperature-dependent. A linearisation analysis as presented in the previous section (Eqn. (2)) can be used to separate each element in terms of a nominal component and an uncertain component.

Example 1 (contd.): Linearising Eqn. (3) around the operating point $x = x_0 = \alpha/\gamma$,

$$\delta\dot{x} = -\gamma\delta x,$$

where $\delta x = x - x_0$. The parameter γ can be separated into its nominal and uncertain components, respectively, γ_0 and $\Delta\gamma$,

$$\begin{aligned}
\delta\dot{x} &= -\gamma_0\delta x + w, \\
z &= d_\gamma\delta x, \\
w &= \delta_\gamma z,
\end{aligned}$$

where $d_\gamma = \max(\Delta\gamma)$ and $|\delta_\gamma| \leq 1$. This can be represented as a feedback uncertainty (Fig. 2a., inset). The transfer function from the initial condition to δx is

$$P(s) = \frac{1}{s+\gamma} = P_0(s)\frac{1}{1+\Delta\gamma P_0(s)},$$

where the nominal transfer function is $P_0(s) = \dfrac{1}{s+\gamma_0}$.

To get a bound on the transfer function,

$$\begin{aligned}
\left|\frac{P(j\omega)}{P_0(j\omega)}\right| &= \sqrt{\frac{\omega^2+\gamma_0^2}{\omega^2+(\gamma_0+\Delta_\gamma)^2}}, \\
\Rightarrow 5\sqrt{\frac{\omega^2+\gamma_0^2}{25\omega^2+36\gamma_0^2}} \leq \left|\frac{P(j\omega)}{P_0(j\omega)}\right| &\leq 5\sqrt{\frac{\omega^2+\gamma_0^2}{25\omega^2+16\gamma_0^2}}.
\end{aligned}$$

We compared these bounds with Monte Carlo simulations of the magnitude of transfer function (Fig. 2a.). Both the upper and lower bounds are conservative work well. In particular, the uncertainty almost vanishes as frequency increases. This is consistent with our expectation as for large enough frequency, the upper bound is unity. The reason this happens is because even when parameter uncertainty is the largest possible, it does not affect the dynamics in the higher frequency range. This graphical uncertainty representation highlights this point. □

As a similar exercise may be performed for *Example 2*, we proceed to the example of the feedforward loop.

Example 3 (contd.): Linearising Eqn. (5) around the operating point $u = u_0$, $x = x_0 = \alpha_x u_0/\gamma$, and $y = y_0$,

$$\begin{bmatrix} \delta\dot{x} \\ \delta\dot{y} \end{bmatrix} = \begin{bmatrix} a_{11} & 0 \\ a_{21} & a_{11} \end{bmatrix}\begin{bmatrix} \delta x \\ \delta y \end{bmatrix} + \begin{bmatrix} b_1 \\ b_2 \end{bmatrix}\delta u, \quad (6)$$

where $\delta x = x - x_0$, $\delta y = y - y_0$, and $\delta u = u - u_0$. The matrix components are $a_{11} = -\gamma$, $a_{21} = -\alpha_y u_0 K_x/x_0^2 = -y_0\gamma/u_0/\alpha_x$, $b_1 = \alpha_x$, and $b_2 = \alpha_x K_x/x_0 = y_0\gamma/u_0$. Using a procedure based on Eqn. (2), each of these elements may be separated into their nominal and uncertain components: $a_{11,0} = -\gamma_0$, $\Delta a_{11} = \Delta\gamma = \pm\gamma_0/5$; $a_{21,0} = -y_{0,0}\gamma_0/(u_0\alpha_{x,0})$, $\Delta a_{21} = \Delta y_0\gamma_0/(u_0\alpha_{x,0}) + \Delta\gamma_0 y_{0,0}/\alpha_{x,0} + y_{0,0}\gamma_0/\alpha_{x,0}^2\Delta\alpha_x$; $b_{1,0} = \alpha_{x,0}$, $\Delta b_1 =$

$\Delta\alpha_x = \pm\alpha_{x,0}/5$; $b_{2,0} = y_{0,0}\gamma_0/u_0$, $\Delta b_2 = y_{0,0}\Delta\gamma + \gamma_0\Delta y_0$. After separating the uncertainty,

$$\begin{bmatrix} \delta\dot{x} \\ \delta\dot{y} \end{bmatrix} = \begin{bmatrix} a_{11,0} & 0 \\ a_{21,0} & a_{22,0} \end{bmatrix}\begin{bmatrix} \delta x \\ \delta y \end{bmatrix} + \begin{bmatrix} b_{1,0} \\ b_{2,0} \end{bmatrix}\delta u + \begin{bmatrix} 1 & 0 & 0 & -1 & 0 \\ 0 & 1 & 1 & 0 & -1 \end{bmatrix}\begin{bmatrix} w_1 \\ w_2 \\ w_3 \\ w_4 \\ w_5 \end{bmatrix},$$

$$\begin{bmatrix} z_1 \\ z_2 \\ z_3 \\ z_4 \\ z_5 \end{bmatrix} = \begin{bmatrix} 0 & 0 \\ 0 & 0 \\ d_{a21} & 0 \\ d_{a11} & 0 \\ 0 & d_{a11} \end{bmatrix}\begin{bmatrix} \delta x \\ \delta y \end{bmatrix} + \begin{bmatrix} d_{b1} \\ d_{b2} \\ 0 \\ 0 \\ 0 \end{bmatrix}\delta u,$$

$$\begin{bmatrix} w_1 \\ w_2 \\ w_3 \\ w_4 \\ w_5 \end{bmatrix} = \begin{bmatrix} \delta_{b1} & 0 & 0 & 0 & 0 \\ 0 & \delta_{b2} & 0 & 0 & 0 \\ 0 & 0 & \delta_{a21} & 0 & 0 \\ 0 & 0 & 0 & \delta_{a11} & 0 \\ 0 & 0 & 0 & 0 & \delta_{a11} \end{bmatrix}\begin{bmatrix} z_1 \\ z_2 \\ z_3 \\ z_4 \\ z_5 \end{bmatrix},$$

where $d_{a11} = \max(\Delta a_{11})$, $d_{a21} = \max(\Delta a_{21})$, $d_{b1} = \max(\Delta b_1)$, $d_{b2} = \max(\Delta b_2)$, $|\delta_{b1}| \leq 1$, $|\delta_{b2}| \leq 1$, $|\delta_{a11}| \leq 1$, and $|\delta_{a21}| \leq 1$. This uncertainty representation belongs to the class of feedback uncertainty (Fig. 2b., inset).

To obtain a graphical representation, a similar exercise, of separating out the uncertainty components, may be performed in terms of the transfer function from δu to δy. The transfer function is

$$P(s) = \frac{y_0}{u_0}\frac{\gamma s}{(s+\gamma)^2} = P_0(s)\frac{(1+\frac{\Delta\gamma}{\gamma_0})(1+\frac{\Delta_{y_0}}{y_{0,0}})}{(1+\frac{\Delta\gamma}{s+\gamma_0})^2},$$
$$\text{where } P_0(s) = \frac{y_{0,0}}{u_0}\frac{\gamma_0 s}{(s+\gamma_0)^2}$$

is the nominal transfer function. This expression can be rearranged to get a bound on the magnitude of the actual transfer function in terms of the nominal transfer function,

$$\left|\frac{P(j\omega)}{P_0(j\omega)}\right| = \left(\left|1+\frac{\Delta\gamma}{\gamma_0}\right|\left|1+\frac{\Delta_{y_0}}{y_{0,0}}\right|\right)\frac{\omega^2+\gamma_0^2}{\omega^2+(\gamma_0+\Delta_\gamma)^2},$$
$$\Rightarrow \left|\frac{P(j\omega)}{P_0(j\omega)}\right| \leq \left(1+\frac{|\Delta\gamma|}{\gamma_0}\right)\left(1+\frac{|\Delta_{y_0}|}{y_{0,0}}\right)\frac{\omega^2+\gamma_0^2}{\omega^2+(\gamma_0+\Delta_\gamma)^2},$$
$$\&\left|\frac{P(j\omega)}{P_0(j\omega)}\right| \geq \left|1-\frac{|\Delta\gamma|}{\gamma_0}\right|\left|1-\frac{|\Delta_{y_0}|}{y_{0,0}}\right|\frac{\omega^2+\gamma_0^2}{\omega^2+(\gamma_0+\Delta_\gamma)^2},$$
$$\Rightarrow 2\frac{\omega^2+\gamma_0^2}{25\omega^2+36\gamma_0^2} \leq \left|\frac{P(j\omega)}{P_0(j\omega)}\right| \leq 57\frac{\omega^2+\gamma_0^2}{25\omega^2+16\gamma_0^2}.$$

We compared these bounds with those obtained from the Monte Carlo simulations of the magnitude of transfer function (Fig. 2). Overall, we find that both the upper and lower bounds are conservative, with the lower bound being more so. In particular, the upper bound is tight towards the higher frequency range. In this range, it is the numerator of the transfer function which has dominant effect in the uncertainty. These bounds help to estimate variation in the peak of the transfer function. □

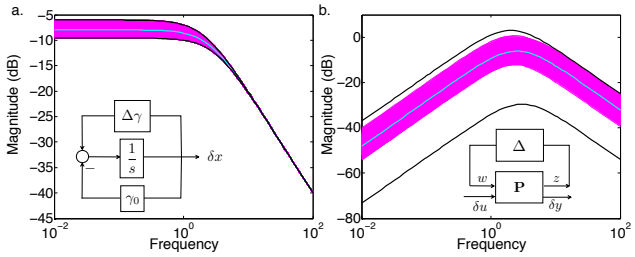

Fig. 2. Uncertainty bounds for linearised dynamics for a. Production-degradation circuit model and b. Incoherent Feedforward Loop circuit model. Magenta lines represent the magnitude of the transfer function of a number of random simulations. Cyan line represents the nominal transfer function. Black lines represent the uncertainty bounds obtained from a linearised analysis. Insets are block diagram representations of the uncertainty.

In this section, we have applied the standard uncertainty representation from linear control theory for the case of temperature uncertainty. For these cases, they show how temperature can be represented as a feedback uncertainty and hoe a bound on the frequency-domain characteristics may be estimated.

IV. UNCERTAINTY IN TRAJECTORIES

Finally, we consider the bounding the variation in the time trajectory. There are at least two cases in which this is possible. One, when the exact solution of the time trajectory is available from the nonlinear dynamical equations. Two, when the exact time trajectory is approximated by the solution of the corresponding linearised system of equations. In both these cases, we have, $x = x(t,\mu)$, where t is time. Linearising this for the nominal parameters $\mu_0 \Rightarrow \Delta x(t) = \frac{\partial x}{\partial \mu}\Delta\mu$, where the partial derivative is evaluated on the nominal trajectory $x(t,\mu_0)$. Then, uncertainty in each component of the state vector can be estimated as $|\Delta x_i(t)| \leq \sum_j [\frac{\partial x}{\partial \mu}]_{ij}|\Delta\mu_j|$. We note that the uncertainty in the time trajectory can vary with time.

Example 1 (contd.): The time trajectory starting from zero initial condition of the nonlinear dynamics (Eqn. (3)) is $x(t) = x_0(1-e^{-\gamma t})$. From the above framework, the uncertainty in this trajectory is estimated to be,

$$|\Delta x(t)| = (1-e^{-\gamma_0 t})\Delta x_0 + x_0 t e^{-\gamma_0 t}\Delta\gamma.$$

Overall, these compare reasonably well with the performance variation observed in Monte Carlo simulations of the complete system dynamics(Fig. 3a.). Analogous to the case observed for the steady-state variation (Fig. 1a.), the upper bound is a slight underestimate and the lower bound is an overestimate. □

Example 3 (contd.): The time trajectory for a step input through the linearised dynamics Eqn. (6) is $\delta y(t) = (y_0/u_0)\gamma t e^{-\gamma t}$. Using the above framework, the uncertainty

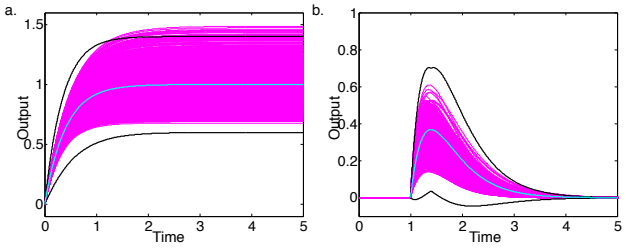

Fig. 3. Uncertainty bounds for trajectories. a. Production-degradation circuit model. Magenta lines represent the trajectories computed from the nonlinear system of equations Eqn. (3) for randomly selected parameters. Cyan line represents the trajectory from the nominal system. Black lines represent the uncertainty bounds obtained from analysis of the linearised dynamics. b. Incoherent Feedforward Loop circuit model. Magenta lines represent the trajectories the deviation from the steady-state computed from the nonlinear system of equations Eqn. (5) for randomly selected parameters. Cyan and black lines are as above.

in this trajectory is,

$$\begin{aligned} \Delta\delta y(t) &= \frac{\gamma_0 t e^{-\gamma_0 t}\Delta y_0 + y_{0,0} t e^{-\gamma_0 t}[1-\gamma_0 t]\Delta\gamma}{u_0}, \\ \Rightarrow |\Delta\delta y(t)| &\leq \frac{\gamma_0 t e^{-\gamma_0 t}|\Delta y_0| + y_{0,0} t e^{-\gamma_0 t}|1-\gamma_0 t||\Delta\gamma|}{u_0}, \\ &= \delta y(t)_0 \Big(\frac{|\Delta y_0|}{y_{0,0}} + |1-\gamma_0 t| \frac{|\Delta\gamma|}{\gamma_0} \Big). \end{aligned}$$

We compared this bound with deviation from the steady-state from Monte Carlo simulations of the nonlinear equations (Eqn. (5)). In this way, the variation in trajectory can be bounded (Fig. 3b.). Both bounds are conservative. The upper bound is reasonably tight for the rising portion of the trajectories, consistent with its behaviour in the high frequency range of the plots. In particular, this can be used to estimate the time-domain properties such as pulse height and pulse width. The lower bound is the more conservative of the two. In particular, those times where it is negative may just be replaced with 0, given the positivity constraint of the concentration variables. □

Based on these examples, we find that this approach provides a way to estimate analytical performance bound for the time trajectories as well as some of their properties.

V. CONCLUSIONS

Assessing robustness of biomolecular circuit function to uncertainty in circuit parameters, for example, due to temperature, is an important problem. Using tools of uncertainty representation from control theory on examples of biomolecular circuits exhibiting dynamic behaviour, we present three results. One, we calculate worst-case performance bounds for steady-state uncertainty for a given temperature uncertainty. Two, we consider dynamics of the linearisation around the steady-state, find that temperature uncertainty can be represented as a feedback uncertainty, and bound variations in the transfer function. Three, we bound the variation in the system trajectories, both over time as well as for some time-domain attributes. These results provide an analytical framework to estimate variation in performance for a temperature uncertainty.

An interesting aspect we find here, is in the comparison of the bounds, obtained from a standard linearisation analysis, with Monte Carlo simulations where nonlinearities can play a role. Given the infinitesimal nature of validity of any linearisation analysis, it is not strictly expected to hold for the complete nonlinear system. In general, it depends on the nature of nonlinearity and the extent of variation. For the parameter uncertainties considered here, the match is reasonably good. In particular, the upper bound is found to be closer to the Monte Carlo simulation than the lower bound. Further the upper bound for the transfer function magnitude works particularly well for the high frequency dynamics.

An important direction for future work is to compare these performance bounds with those obtained from other methods. The performance bounds developed here for biomolecular circuits, often intrinsically nonlinear systems. For such nonlinear systems in engineering contexts, there have been investigations to formulate the robustness analysis as an optimisation problem [17]. In this approach, worst-case bounds are obtained by optimising over a parameter uncertainty interval for the output of interest. Comparing bounds obtained from these methods to the presented bounds as well as the Monte Carlo simulations should further clarify the variation in performance due to temperature uncertainty.

Uncertainty representations in control engineering contexts allow a determination of robustness in stability and in performance. Here, we have developed a framework for representing temperature uncertainty in biomolecular circuits, and estimating quantitative performance bounds due to it. Given that one of the motivations for uncertainty representations in control theory is to conveniently represent nonlinear dynamical behaviours for ease of analysis and design, a systematic analysis of this approach for temperature uncertainty in biomolecular circuits, as presented here, highlights different aspects of the process. Further, this should be useful for assessing performance robustness for biomolecular circuits. Finally, this should be useful in a relatively quick comparison, especially as system dimensions increase, of the effect of different controllers on the performance of biomolecular circuits.

REFERENCES

[1] Mackenroth, Uwe, *Robust Control Systems: Theory and Case Studies*. Springer-Verlag, 2004.
[2] L. Ma and P. A. Iglesias, "Quantifying robustness of biochemical network models," *BMC Bioinformatics*, vol. 3, p. 38, Dec. 2002.
[3] J. Kim, D. Bates, I. Postlethwaite, L. Ma, and P. Iglesias, "Robustness analysis of biochemical network models," *IEE Proceedings - Systems Biology*, vol. 153, no. 3, p. 96, 2006.
[4] J. E. Shoemaker and F. J. Doyle, "Identifying fragilities in biochemical networks: robust performance analysis of Fas signaling-induced apoptosis," *Biophys. J.*, vol. 95, no. 6, pp. 2610–2623, Sept. 2008.
[5] S. Waldherr and F. Allgöwer, "Robust stability and instability of biochemical networks with parametric uncertainty," *Automatica*, vol. 47, no. 6, pp. 1139–1146, June 2011.
[6] N. Barkai and S. Leibler, "Robustness in simple biochemical networks," *Nature*, vol. 387, no. 6636, pp. 913–917, June 1997.
[7] A. Eldar, R. Dorfman, D. Weiss, H. Ashe, B.-Z. Shilo, and N. Barkai, "Robustness of the BMP morphogen gradient in Drosophila embryonic patterning," *Nature*, vol. 419, no. 6904, pp. 304–308, Sept. 2002.

[8] S. Sen and R. M. Murray, "Temperature dependence of biomolecular circuit designs," in *52nd IEEE Conference on Decision and Control*, Dec. 2013, pp. 1398–1403.

[9] S. Sen, J. Kim, and R. M. Murray, "Designing robustness to temperature in a feedforward loop circuit," in *53rd IEEE Conference on Decision and Control*, Dec. 2014, pp. 4629–4634.

[10] A. B. Reyes, J. S. Pendergast, and S. Yamazaki, "Mammalian peripheral circadian oscillators are temperature compensated," *J Biol Rhythms*, vol. 23, pp. 95–98, 2008.

[11] S. Mangan and U. Alon, "Structure and function of the feed-forward loop network motif," *Proc Natl Acad Sci USA*, vol. 100, no. 21, pp. 11 980–11 985, Oct. 2003.

[12] S. S. Shen-Orr, R. Milo, S. Mangan, and U. Alon, "Network motifs in the transcriptional regulation network of Escherichia coli," *Nat Genet*, vol. 31, no. 1, pp. 64–68, May 2002.

[13] W. Ma, A. Trusina, H. El-Samad, W. A. Lim, and C. Tang, "Defining network topologies that can achieve biochemical adaptation," *Cell*, vol. 138, no. 4, pp. 760–773, Aug. 2009.

[14] L. Goentoro, O. Shoval, M. W. Kirschner, and U. Alon, "The incoherent feedforward loop can provide fold-change detection in gene regulation," *Mol Cell*, vol. 36, no. 5, pp. 894–899, Dec. 2009.

[15] O. Shoval, L. Goentoro, Y. Hart, A. Mayo, E. Sontag, and U. Alon, "Fold-change detection and scalar symmetry of sensory input fields," *Proc Natl Acad Sci USA*, vol. 107, no. 36, pp. 15 995–16 000, Sept. 2010.

[16] J. J. Tyson, K. C. Chen, and B. Novak, "Sniffers, buzzers, toggles and blinkers: dynamics of regulatory and signaling pathways in the cell," *Curr Opin Cell Biol*, vol. 15, no. 2, pp. 221–231, Apr. 2003.

[17] J. E. Tierno, R. M. Murray, J. C. Doyle, and I. M. Gregory, "Numerically Efficient Robustness Analysis of Trajectory Tracking for Nonlinear Systems," *Journal of Guidance, Control, and Dynamics*, vol. 20, no. 4, pp. 640–647, July 1997.